




Research Article

Comparative Evaluation for Selected Gas Turbine Cycles

^{1*}Mohamed Elwardany , ²Abd El-Moneim M. Nassib , ³Hany A. Mohamed 

^{1,2,3} Department of Mechanical Power Engineering, Faculty of Engineering, Assiut University, Assiut 71516, Egypt

³ Manufacturing Department, Modern Academy for Engineering and Technology, Cairo 11571, Egypt

E-mail: ^{1*} M.Wardany@anu.edu.eg

Received 21 March 2023, Revised 25 August 2023, Accepted 11 September 2023

Abstract

The energy and exergy evaluation of simple gas turbine (SGT), gas turbine with air bottoming cycle (GT-ABC), and partial oxidation gas turbine (POGT) are studied. The governing equations for each cycle are solved using energy equation Solver (EES) software. The characteristics performance for selected cycles are discussed and verified with that obtained for available practical cycles (SGT, GT-ABC, POGT). The present results show a good agreement with the practical one. The effects of significant operational parameters, turbine inlet temperature (TIT), compression ratio (CR), and compressor inlet temperature (CIT), on the specific fuel consumption, energy and exergy efficiencies are discussed. According to the findings, a reduction in CIT and a rise in TIT and CR led to enhance energy and exergy efficiency for each configuration with different ranges. Results revealed that the GT-ABC and POGT cycles are more efficient than those of SGT at the same operational parameters. The energy and exergy efficiencies are 38.4%, 36.2% for SGT, 40%, 37.8 % for GT-ABC, and 41.6%, 39.3% for POGT. The POGT cycle has a better energy and exergy performance at a lower pressure ratio than the SGT and GT-ABC.

Keywords: Gas turbine; thermal analysis; energy; exergy; efficiency.

1. Introduction

Energy consumption is a critical development metric, driven by factors such as population growth, urbanization, industrialization, and technological advancements. This surge in energy demand, primarily met by fossil fuels accounting for 80% of electricity generation, has led to environmental issues, including pollution and the greenhouse effect [1]. Global electricity demand is rising at an annual rate of approximately 6% [2], with fossil fuels, particularly natural gas (NG), contributing significantly to CO₂ emissions [3]. NG presently constitutes 22% of global primary energy production and is projected to increase its share in electricity generation by 2040, reaching 28% from 22% in 2012 [4]. The concept of "analysis of thermal power plants" encompasses the effective utilization of energy resources. Prior to 1940, the energy efficiency of power plants was assessed using the first law of thermodynamics, while exergy analysis, based on the second law, has since offered insights into energy losses, aiding in the design, evaluation, optimization, and enhancement of thermal power plants [5]–[8].

Exergy analysis stands out as an effective technique for optimizing energy systems by offering an intricate understanding of a system's thermodynamic performance. This analytical approach proves invaluable in pinpointing areas ripe for enhancement and fine-tuning the operation and design of energy systems, leading to heightened efficiency, reduced energy consumption, and a diminished environmental footprint. A standout advantage of exergy assessment lies in its ability to provide a comprehensive overview

of energy flows and losses within a system. By discerning the exergy destruction within each component of a system, engineers gain the insights necessary to identify energy losses and develop strategies to curtail them. This, in turn, paves the way for significant strides in energy efficiency and cost reduction. Exergy analysis also facilitates the optimization of energy systems under various operational conditions [9]–[12].

Significant energy losses to the ecosystem arise from incomplete combustion processes and the rapid expansion of high-temperature, high-pressure exhaust gases, resulting in environmental pollution and contributing to global warming [10],[11]. A study by Ibrahim et al.[15] studied simplified gas turbine model through energy and exergy assessments found that the combustion chamber was the primary locus of exergy destruction. The air compressor exhibited energy and exergy efficiencies of 92% and 94.9%, respectively. In comparison, the combustion chamber demonstrated energy and exergy efficiencies of 61.8% and 67.5%, in contrast to the 82% and 92% efficiencies of gas turbines. The combined energetic and exergetic efficiencies were calculated at 34.3% and 32.4%, respectively. Kurt et al. [16] investigated various operational parameters of gas turbine power plants and determined that the highest overall power output occurred at TIT=1600K, CIT=288.15 K, and PR=22 when analyzed for turbine inlet temperature (TIT), compressor inlet temperature (CIT), and pressure ratio (PR). Conversely, it peaked at CIT=273.15K, TIT=1423.15 K, and PR=18 when considering compressor inlet temperature. Sa et al. [17] proposed an empirical relationship regarding a gas turbine's capacity to generate electricity under ambient air conditions

differing from ISO standards. Their findings, derived from over 8,000 data readings across approximately 280 days of gas turbine operation, indicated that for each degree increase in ambient temperature beyond ISO conditions, the gas turbine experienced a 1.47 MW power output reduction and a 0.1% decline in thermal efficiency.

Abou Al-Sood et al. [18] provided insights into the operational performance of a gas turbine employing an irreversible intercooler, regenerative, and reheat gas cycle. Optimization studies unveiled that the lowest temperature ranged from 302 K to 315 K, while the highest temperature fluctuated between 1320 K and 1360 K. To maximize performance parameters, the cycle's highest pressure was found to be optimal within the range of 1449 kPa to 2830 kPa. On a related study, Aydin [19] introduced exergy sustainability indicators for the assessment of gas turbine power plant operations, considering two distinct configurations. In Case A, based on LM6000 GT technology, the power plant generated 43.3 MW of electricity at full capacity, while Case B, incorporating steam turbine cycles, produced 54.3 MW. The addition of the steam cycle led to a 10% reduction in the waste-exergy ratio. In both cases, the power plants exhibited recoverable exergy ratios of approximately 22% and 13.1%, respectively. Notably, the environmental impact factor improved by about 50% in the scenario of the steam cycle power plant (Case B). Ultimately, the exergetic sustainability indices for Case A and Case B power plant configurations were calculated at 0.651 and 0.978, respectively, reflecting their sustainability and efficiency.

In the late 1980s, an Air Bottoming Cycle (ABC) emerged as a viable alternative to the conventional steam bottoming cycle, which utilizes hot combustion products for heat in the bottoming cycle [20]. Carcasci et al. [20] conducted an investigation into an ABC system integrated with an industrial medium-power gas turbine. The results revealed that this gas turbine, when coupled with the ABC, exhibited enhanced power output and higher thermal efficiency compared to a standalone gas turbine. Notably, the primary GE10 turbine's thermal efficiency experienced a notable increase of 7.6%, while its output power surged by 22.3%. Ghazikhani et al. [21] further delved into the exergy aspects of a simple gas turbine versus a GT-ABC configuration. Their findings indicated that exhaust exergy recovery in the GT-ABC ranged from 8.6% to 14.1% of the fuel exergy, depending on operating conditions, while only 4.7% to 7.4% of the fuel exergy was lost due to the added components in the ABC. The specific fuel consumption (SFC) of the GT-ABC was generally 13.3% lower, and the specific work was 15.4% higher compared to the simple gas turbine. Alklaibi et al. [14] conducted a comparative analysis of the GT-ABC against simple and modified gas turbines, examining the influence of bottoming and topping cycle pressure ratios on work output and thermal efficiency. They found that at peak efficiency, the simple gas turbine cycle with ABC improved efficiency by 4.78%. An exergy analysis revealed that a gas turbine bottoming cycle reduced overall exergy destruction by 6%. Notably, the loss of exergy in the exhaust gas of a conventional gas turbine accounted for 47% of the overall exergy destruction, a figure reduced to 31% when implementing a GT-ABC system. Graziani et al. [22] explored the impact of ambient temperature on the exergy destruction of a GT-ABC, observing a 6% average improvement in second-law efficiency when adding a heat exchanger to a basic gas turbine to recover exhaust exergy

despite maintaining identical inlet air temperatures in both cycles.

Gas turbines have been the subject of cycle enhancements because the traditional Brayton cycle has inherent limitations in terms of efficiency and emissions improvement. To address these challenges, various enhancements such as recuperation, intercooling, reheat, and water/steam injection have been incorporated into cycle performance studies. These modifications aim to facilitate more complete fuel combustion. One innovative approach is the use of Partial Oxidation Gas Turbines (POGT), which employ a partial oxidation reactor instead of a conventional combustor, requiring stoichiometric air-fuel ratios. POGT benefits from a higher specific heat compared to complete combustion [23], [24]. This technology results in a remarkable 10% increase in system efficiency compared to a standard gas turbine bottoming cycle. These efficiency gains can be attributed to several factors, including nearly isothermal expansion, reduced density of partial oxidation products, increased volumetric gas flow in the turbine (15-20%), and significantly lower airflow requirements, typically 65% less than those of a conventional expansion turbine [23].

In their study, Diyoke et al. [25] conducted a comprehensive evaluation of a hybrid gas turbine and biomass power system with the aim of promoting sustainable multi-generation practices in Nigeria. They introduced two distinct configurations of this hybrid system, which coupled a Gas Turbine Combined Cycle (GTC) with a Biomass Power System (BPS) integrated with an Absorption Refrigeration System (ARS) to facilitate Combined Cooling, Heating, and Power (CCHP) generation. Configuration 1 and Configuration 2 exhibited overall exergy efficiencies estimated at approximately 17% and 19%, respectively. Notably, among the various system components, the biomass gasifier contributed the most to exergy destruction (87%), followed by the combustion chamber (5.5%) and the syngas engine generator (3%). Their emission analysis revealed that these hybrid systems emitted roughly 30% less CO₂ in comparison to a standard recuperated GTC of equivalent capacity.

Additionally, the Levelized Cost of Electricity (LCOE) for the first and second proposed systems was calculated at 0.1373 and 0.1328 \$/kWh, respectively, highlighting their potential advantages in terms of multiple output capabilities and CO₂ emission reduction. This innovative approach combines biomass and natural gas resources for enhanced sustainability. In a separate study, Fan et al. [26] conducted a comparative investigation into the design and performance of innovative cascade CO₂ combined cycles for harnessing waste heat from gas turbine (GT) exhaust. They introduced a novel two-stage cascaded supercritical CO₂ and transcritical CO₂ (sCO₂-tCO₂) power cycle for waste heat recovery (WHR) from GT exhaust. Simulation results demonstrated that the SSBC-tCO₂ cycle outperformed the RSBC-tCO₂ cycle in its suitability as a bottoming cycle for GT, owing to its ability to generate higher power with a simpler configuration. Compared to traditional GT-RSBC and GT-SSBC setups, the optimal GT-CCO₂ cycle (GT-SSBC-tCO₂) exhibited significant improvements of 5.32% and 4.32% in thermal efficiency, showcasing its potential for enhancing energy efficiency and waste heat utilization in gas turbine systems.

Ryu et al. [27] conducted a comparative assessment of integrated solid oxide fuel cell-gas turbine (SOFC-GT)

systems for marine vessels, using ammonia and hydrogen as fuels. They used Aspen HYSYS V.12.1 for system design and modeling, analyzing it based on the first and second laws of thermodynamics. Direct ammonia and hydrogen SOFCs achieved energy efficiencies of 60.96% and 64.46%, respectively. Combining the systems increased energy efficiencies by 12.37% and 13.97% when using ammonia and hydrogen, compared to single SOFC systems. The study also examined exergy destruction in primary system components and determined the most suitable fuel utilization factor. This analysis highlights ammonia as a hydrogen carrier and emphasizes waste heat recovery for enhancing SOFC system performance.

In this study, we evaluated the energy and exergy performance of selected gas cycles (SGT, GT-ABC, POGT) under the same operation and design parameters. We used EES to simulate data and assess the impact of environmental conditions and other factors on cycle performance. Data were based on prior literature for each model.

2. Modelling and Analysis

2.1 Energy Analysis

The energy evaluations of the gas turbine cycle are related to the Brayton cycle. The computation will include evaluating the input and output energy of the system. The primary components of the gas turbine cycle include air compressors, combustion chamber, and gas turbine. Following are the equations required for analyzing each component of the gas turbine cycle [7].

Compressor:

$$T_2 = T_1 \left(1 + \frac{1}{\eta_{AC}} \left(r_{AC}^{\frac{k-1}{k}} - 1 \right) \right) \quad (1)$$

$$\dot{W}_{AC} = \dot{m}_a c_{pa} (T_2 - T_1) \quad (2)$$

$$c_{pa}(T) = 1.048 - \left(\frac{1.83T}{10^4} \right) + \left(\frac{9.45T^2}{10^7} \right) - \left(\frac{5.49T^3}{10^{10}} \right) + \left(\frac{7.92T^4}{10^{14}} \right) \quad (3)$$

In equation. (1), T_1 and T_2 represent the air temperature at the compressor input and discharge sections, k is the specific heat ratio, and r is the compression ratio. The power consumption of the compressor is calculated using equation (2). Equation (3) provides the air specific heat depending on the varying temperatures.

Combustion chamber:

$$\dot{m}_a h_2 + \dot{m}_f \text{LHV} = \dot{m}_g h_3 + (1 - \eta_{cc}) \dot{m}_f \text{LHV} \quad (4)$$

$$\dot{m}_g = \dot{m}_f + \dot{m}_a \quad (5)$$

$$f = \frac{\dot{m}_f}{\dot{m}_a} \quad (6)$$

Fuel air ratio is illustrated in equation (6). Lower heating value (LHV) differs based on the characteristics of the fuel used. This analysis employs natural gas (NG) in the combustion chamber. Chemically, NG is mostly methane (CH₄), about 75% to 99% of the gas; however, small quantities of other hydrocarbons can also be found in natural gas, along with carbon dioxide, hydrogen, nitrogen, carbon monoxide, and hydrogen sulfide [28].

Gas turbine:

$$T_4 = T_3 \left(1 - \eta_{GT} \left(1 - \left(\frac{P_3}{P_4} \right)^{\frac{k-1}{k}} \right) \right) \quad (7)$$

$$\dot{W}_{GT} = \dot{m}_g c_{p,g} (T_{A_3} - T_{A_4}) \quad (8)$$

$$c_{p,g}(T) = 0.991 + \left(\frac{6.997T}{10^5} \right) + \left(\frac{2.712T^2}{10^7} \right) - \left(\frac{1.2244T^3}{10^{10}} \right) \quad (9)$$

In equation. (7), T_3 and T_4 represent the turbine input and output combustion gas temperatures, respectively.

Power output from the turbine is calculated using equation (8). Equation (3) evaluates the specific heat of air based on varying temperature.

2.2 Exergy Analysis

Exergy is the maximum useful work achieved as a system reaches equilibrium with its surroundings. Utilizing the second law of thermodynamics, mass and energy balances, exergy analysis is an effective technique for evaluating the performance of energy systems. Exergy includes four components: chemical, physical, kinetic, and potential exergies. Only chemical and physical exergies are accounted for in the analyses, while kinetic and potential exergy are ignored. Physical exergy shows the maximum work capacity of a system. In contrast, chemical exergy is related to a system's chemical composition variation from equilibrium conditions [29]. General exergy analysis equations are shown below:

$$\dot{E}_{x, \text{heat}} + \sum_i \dot{m}_i e_{x,i} = \sum_e \dot{m}_e e_{x,e} + \dot{E}_{x,w} + \dot{I}_{\text{dest}} \quad (10)$$

$$\dot{E}_{x,w} = \dot{W} \quad (11)$$

$$\dot{E}_{x, \text{heat}} = \left(1 - \frac{T_o}{T_i} \right) \dot{Q}_i \quad (12)$$

$$\dot{E}_x = \dot{E}_{x, \text{phy}} + \dot{E}_{x, \text{che}} \quad (13)$$

Using equation. (10), the exergy flow rate for each system component can be determined [30]. Equation. (11) demonstrates the work performed by the system from exergy flow [30]. The rate of exergy generation with heat is shown in equation (12) [30]. The physical and chemical exergies of the component are shown in equation (13) [30].

The physical exergy is produced due to the system deviation from its dead state condition in terms of pressure and temperature [15]. Use the following equations to calculate the system physical exergy [46].

$$e_x = e_{x, \text{phy}} + e_{x, \text{che}} \quad (14)$$

$$e_{x, \text{phy}} = e_x^T + e_x^P \quad (15)$$

$$e_x^T = c_p \left((T - T_o) - T_o \ln \frac{T}{T_o} \right) \quad (16)$$

$$e_x^p = RT_o \ln \frac{P}{P_o} \quad (17)$$

The physical exergy calculation is shown in equation (15). Equations (16) and (17) determine physical exergy based on temperature and pressure. P_o and T_o represent the surrounding pressure and temperature, whereas C_p and R denote the specific heat at constant pressure and gas constant, respectively [30].

Chemical exergy is caused when the chemical composition of the system deviates from the surrounding dead-state condition [15]. The following equation can be used to determine the exergy flow of the fuel.

$$\xi = \frac{e_{x, \text{fuel}}}{LHV_{\text{fuel}}} \quad (18)$$

According to equation (18), ξ represents the ratio of exergy flow to the LHV of the fuel. ($LHV_{\text{fuel}} = 48,806 \text{ KJ/kg}$) Usually, the value for ξ is 1.06 for NG [15]. Thus, the value of fuel exergy can be calculated using the ratio of exergy and the LHV. The following equation can be used to determine the exergy of the combustion products [15].

$$e_{x, \text{cg}} = \frac{[\sum_{i=1}^n x_i e_{x, \text{che}, i} + RT_o \sum_{x=1}^n x_i \ln(x_i)]}{\sum(x_i)} \quad (19)$$

The subscripts I in equation (19) identify the type of air fraction, x is the molar fraction of air, and $e_{x, \text{che}}$ is the standard chemical exergy of each component of air fraction. Table 1 contains the Standard chemical exergy and molar fraction of each gas. The following equations can achieve a more accurate result [31].

$$\lambda = \frac{0.058 \dot{m}_{\text{air}}}{\dot{m}_{\text{fuel}}} \quad (20)$$

$$x_{N_2} = \frac{(7.524)\lambda}{1 + (9.6254)\lambda} \quad (21)$$

$$x_{O_2} = \frac{2(\lambda - 1)}{1 + (9.6254)\lambda} \quad (22)$$

$$x_{CO_2} = \frac{1 + (0.0028)\lambda}{1 + (9.6254)\lambda} \quad (23)$$

$$x_{H_2O} = \frac{2 + (0.0972)}{1 + (9.6254)\lambda} \quad (24)$$

Equations (20 – 24) can compute the molar fraction of each element of the combustion products; the equations are only useful when NG is used as the fuel. Subscript k represents the fuel-air ratio [31].

Table 1. Standard exergy and molar fraction [31].

Element	$e_{x, \text{che}}$ (KJ/mol)	Molar fraction (%)
N_2	0.72	75.67
O_2	3.97	20.34
CO_2	19.87	0.03
H_2O	9.49	3.03

2.3 Exergy Destruction

The product calculations for the exergy flow rate for each part were utilized to determine the exergy destruction. After

each process, the exergy flow will practically decrease. Usually, exergy destruction can be calculated by equation (25) [30].

$$\dot{E}_{x, \text{in}} - \dot{E}_{x, \text{out}} = \dot{E}_{x, D} \quad (25)$$

Air Compressor

$$\dot{E}_{x, D, AC} = \dot{E}_{x_1} - \dot{E}_{x_2} + \dot{W}_{AC} \quad (26)$$

Combustion chamber

$$\dot{E}_{x, D, CC} = \dot{E}_{x_2} + \dot{E}_{x_5} - \dot{E}_{x_3} \quad (27)$$

Gas turbine

$$\dot{E}_{x, D, GT} = \dot{E}_{x_3} - \dot{E}_{x_4} - \dot{W}_{GT} \quad (28)$$

2.4 Component Efficiency

Every component undergoes energy and exergy assessment to identify which has the lowest and highest efficiency. The exergy efficiency can be calculated by the following equation [29].

Air Compressor

$$\eta_{x, AC} = \frac{\dot{E}_{x_2} - \dot{E}_{x_1}}{\dot{W}_{AC}} \quad (29)$$

Combustion chamber

$$\eta_{x, CC} = \frac{\dot{E}_{x_3}}{\dot{E}_{x_3} - \dot{E}_{x_1}} \quad (30)$$

Gas turbine

$$\eta_{x, GT} = \frac{\dot{W}_{GT}}{\dot{E}_{x_3} - \dot{E}_{x_4}} \quad (31)$$

Equation (29) is used to determine the efficiency of the air compressor. Work output and exergy destruction significantly contribute to assessing the efficiency of the air compressor, while the same is true for equation (31), in which the exergy destruction and work output of a gas turbine determine the efficiency. In equation (30), the exergy rate and the exergy destruction for fuel affect the efficiency of the combustion chamber [31]. The equations below can determine the simple gas turbine cycle's overall exergy and energy efficiencies [30].

$$\dot{W}_{\text{net}} = \dot{W}_{GT} - \dot{W}_{AC} \quad (32)$$

$$\text{SFC} = 3600 \frac{\dot{m}_{\text{fuel}}}{\dot{W}_{\text{net}}} \quad (33)$$

$$\eta_I = \frac{\dot{W}_{\text{net}}}{\dot{m}_{\text{fuel}} LHV} \quad (34)$$

$$\eta_{II} = \frac{\dot{W}_{\text{net}, GT}}{\dot{E}_{x, f}} \quad (35)$$

Equation (33) shows the specific fuel consumption for the gas turbine. Equation (35) shows the overall exergy efficiency. Subscript $\dot{E}_{x, f}$ Denotes the fuel exergy

flow rate, while equation (34) shows the overall energy efficiency of the cycle [30].

2.5 Simple Gas Turbine (SGT)

As illustrated in Figure 1. Air is compressed by the compressor before being combined with fuel and fired in the combustion chamber. The hot combustion exhausts expand through the turbine and generate mechanical work. The exhaust gases are then released from the turbine. The energy produced can be used to generate electricity and operate various industrial machinery.

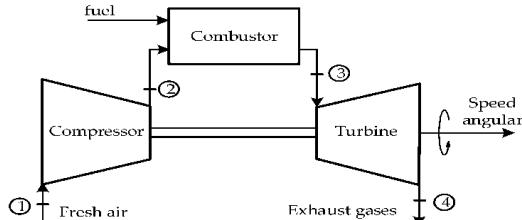


Figure 1. Simple gas turbine (SGT)[32].

The specific fuel consumption, work output, overall energy, and exergy efficiencies for a simple gas turbine cycle can be determined using the equations below [30].

$$\dot{W}_{Net,SGT} = \dot{W}_{GT} - \dot{W}_{AC} \quad (36)$$

$$SFC = 3600 \frac{\dot{m}_{fuel}}{\dot{W}_{net,SGT}} \quad (37)$$

$$\eta_{I,SGT} = \frac{\dot{W}_{net,SGT}}{\dot{m}_{fuel}LHV} \quad (38)$$

$$\eta_{II,SGT} = \frac{\dot{W}_{net,GT}}{\dot{E}_{x,f}} \quad (39)$$

2.6 Gas Turbine with Air Bottoming Cycle (GT-ABC)

A gas turbine with air air-bottoming cycle (GT-ABC) (Figure 2) is a combined cycle that primarily generates electricity from a gas turbine. The gas turbine generates power, while the air bottoming cycle captures and converts exhaust gases into a useful form. Combining a gas turbine with an air-bottoming cycle results in improved efficiency and power production than a single gas turbine. A heat-recovery heat exchanger is the combustion chamber for the bottoming cycle [14].

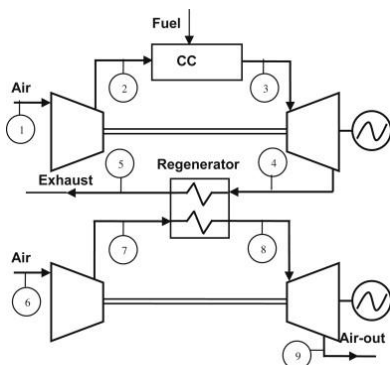


Figure 2. Gas turbine with air bottoming cycle (GT-ABC) [33].

The gas turbine topping cycle was first analyzed based on the details cycle components models described in the

previous section. GT-ABC forms the gas turbine cycle by coupling the air-bottoming with the topping cycle.

The specific fuel consumption, work output, overall energy, and exergy efficiencies for a gas turbine with an air bottoming cycle can be determined using the equations below [30].

$$\dot{W}_{Net,GT-ABC} = \dot{W}_{GT_1} + \dot{W}_{GT_2} - \dot{W}_{AC_1} - \dot{W}_{AC_2} \quad (40)$$

$$SFC = 3600 \frac{\dot{m}_{fuel}}{\dot{W}_{net,GT-ABC}} \quad (41)$$

$$\eta_{I,GT-ABC} = \frac{\dot{W}_{net,GT-ABC}}{\dot{m}_f LHV} \quad (42)$$

$$\eta_{II,GT-ABC} = \frac{\dot{W}_{net,GT-ABC}}{\dot{E}_{x,f}} \quad (43)$$

2.7 Partial Oxidation Gas Turbine (POGT)

A partial oxidation gas turbine (POGT) illustrates in Figure 3, is a specific type of gas turbine that generates electricity using a partial oxidation process. A fuel, such as NG, is burned in a combustion chamber with a restricted quantity of oxygen. This produces a carbon monoxide and hydrogen mixture, subsequently powering the turbine. A gas produced by this cycle has a greater specific heat than a gas produced by complete combustion.

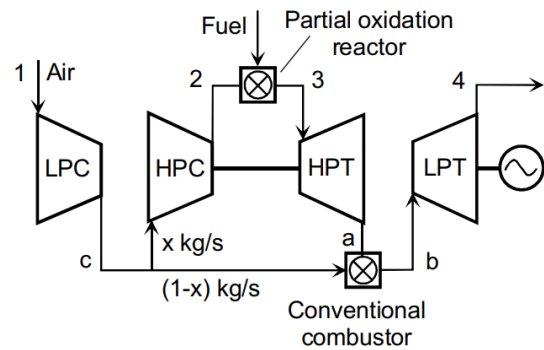


Figure 3. Partial oxidation gas turbine (POGT) [34].

Typically, a Partial oxidation reactor (POR) runs in fuel-rich conditions with equivalency ratios of 2.5. The typical POR exit temperature is between 1093 and 1316°C., in line with turbine inlet requirements [23]. The required turbine inlet temperature T_3 determines fraction x in the PO reaction. For temperatures ranging from 1200 to 1400 °C, x has a value between 0.15 and 0.22. [35].

The following equations can determine the work output, specific fuel consumption, and overall energy and exergy efficiencies for a partial oxidation gas turbine (POGT) [30].

$$\dot{W}_{Net,POGT} = \dot{W}_{HPT} + \dot{W}_{LPT} - \dot{W}_{HPC} - \dot{W}_{LPC} \quad (44)$$

$$SFC = 3600 \frac{\dot{m}_{fuel}}{\dot{W}_{net,POGT}} \quad (45)$$

$$\eta_{I,POGT} = \frac{\dot{W}_{net,POGT}}{\dot{m}_f LHV} \quad (46)$$

$$\eta_{II,POGT} = \frac{\dot{W}_{net,POGT}}{\dot{E}_{x,f}} \quad (47)$$

3. Models Validation

3.1 Simple Gas Turbine (SGT)

Based on the above analysis, a simulation program was developed using EES software [34] for the SGT, GT-ABC, and POGT cycles. The obtained solution for SGT is validated with the results of [15]. Table 3 shows the Operating parameters for the validation process. The comparison between the reference and present models is shown in Table 2, and the model shows a good agreement.

Table 2. Comparison between the Exergy efficiency for all components of simple gas cycle in the present model with [15].

Components	Exergy efficiency (%) present study	Exergy efficiency (%) [15]	Relative error
Air Compressor	88.2	94.9	7.1
Combustion Chamber	73.7	75.3	7.9
Gas Turbine	93.9	94.6	2.5
Power Cycle	29.7	32.3	8.3

3.2 Gas Turbine with Air Bottoming Cycle (GT-ABC)

The findings are compared to the results data taken from [30] and [32] to validate the GT-ABC model. Figure 4 shows the operating parameters used in the validation process for the SFC against turbine inlet temperature for (GT-ABC). As TIT is increased, the SFC decreases. The findings from the developed models showed a good agreement with the published data [30], and [32]. Once the SGT, GT-ABC, and POGT cycle model was developed and validated in EES software, we conducted a comparative parametric analysis.

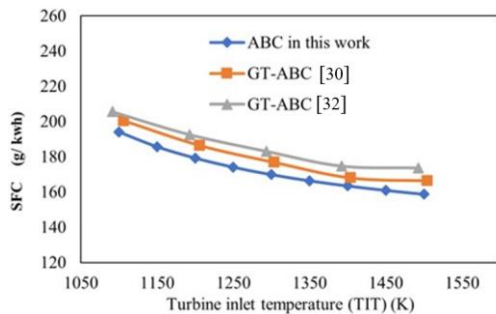


Figure 4. Difference between the results of the gas turbine with air bottoming cycle (GT-ABC) model and those of [33], [36].

4. Results and Discussion

In this study, a comparative analysis of selected gas turbine cycles has been conducted. The conventional energy and exergy analysis for SGT, GT-ABC, and POGT cycles is applied to evaluate the performance of these cycles. The input data for the thermal performance analysis are presented below (Table 3).

Table 4 compares the model findings for overall energy and exergy efficiency and SFC for different cycles. For all systems, the TIT was 1400 °C, and the ambient temperature was 25 °C. The pressure ratio of the topping cycles was 20. The pressure ratio was assumed to be 2 for the bottoming cycles. In POGT, the mass fraction was assumed to be 0.2. The table shows that the GT-ABC and POGT cycles are more efficient than the SGT. Under these conditions, the energy and exergy efficiency are 38.4%, 36.2% for SGT, 40%, 37.8 % for GT-ABC, and 41.6%, 39.3% for POGT. In

addition, the SFC for SGT, GT-ABC, and POGT cycles are 149.5, 136.3, and 177 (g/kwh), respectively.

Table 3. Input data for thermodynamic analysis of SGT, GT-ABC, and POGT [21], [33], [35], [36].

Parameters	Value
Dead state conditions	$P_o = 1.01 \text{ bar}$, $T_o = 293.15 \text{ K}$
Isentropic efficiency of the compressor	85%
Isentropic efficiency of the turbine	87%
Combustion efficiency	98 %
Heat exchanger effectiveness	0.85
Air Mass flow rate, topping cycle	1 kg/s
Air Mass flow rate, bottoming cycle	1 kg/s
Air mass fraction for POGT	0.2
Turbine inlet temperature	900 °C, 1200 °C, 1400 °C
Topping cycle pressure ratio	8, 12, 20
Ambient temperature	5 °C, 25 °C, 35 °C
Compressor inlet pressure	94 kPa
Gasses specific heat	1.14 kJ/kg K
Air Specific heat	1.005 kJ/kg K
Ratio of specific heat for gasses	1.33
Ratio of specific heat for air	1.4
Bottoming cycle pressure ratio	2
Fuel type	NG
Low heating value of NG	48806 kJ/kg

Table 4. The overall energy and exergy efficiencies and SFC for different cycles (TIT = 1400 °C, $T_o = 25 \text{ °C}$, $R_c = 20$, $x = 0.2$ and $rc = 2$).

Cycle type	Energy efficiency (%)	Exergy efficiency (%)	SFC (g/kwh)
SGT	38.4	36.23	149.5
GT-ABC	40.07	37.8	136.3
POGT	41.67	39.31	177

4.1 Effect of Operating Conditions

This section presents the simulation findings of the impact of operating conditions on the performance of the selected gas turbine cycles. The effects of operating parameters on SFC, energy, and exergy efficiencies are conducted using a computer model developed on EES software. The performance of the cycles was assessed under the same operational conditions. The results found are presented in Figure 5 to 11 based on the theoretical relationships earlier mentioned. The plots of the simulations for the SGT, GT-ABC and POGT cycles are presented and analyzed here.

4.1.1 Effect of Turbine Inlet Temperature on Energy and Exergy Efficiencies

The turbine inlet temperature (TIT) has a considerable impact on gas turbine performance. Increasing TIT requires higher SFC, which increases costs and greenhouse gas emissions [37], [38]. The effect of the TIT on the energy and exergy efficiency of each cycle was studied for TIT values ranging from (900 °C to 1400 °C). The findings show that the thermal efficiency increase as the TIT increases, as shown in Figure 5. The graph trend, which seems to align with the available literature data, provides further evidence that the model can determine the actual cycle performance within a reasonable range. Results show that when turbine intake temperatures increase, both exergy and energy efficiencies increase proportionally for all cycles. With varying the TIT,

the energy and exergy efficacies of GT-ABC are higher than SGT and POGT.

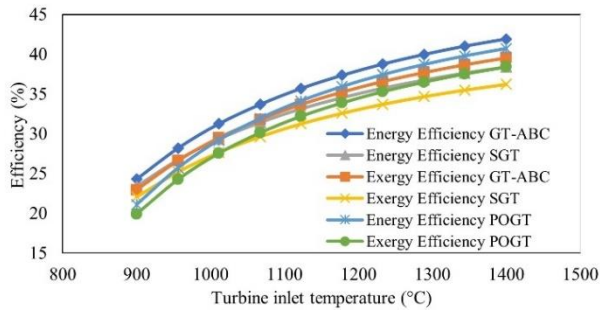


Figure 5. Energy and exergy efficiencies variation against turbine inlet temperature ($R_c = 20$, $T_o = 25^\circ\text{C}$, $x = 0.2$ and $r_c = 2$).

4.1.2 Effect of Turbine Inlet Temperature on Specific Fuel Consumption

Specific fuel consumption (SFC) indicates the quantity of fuel needed for power production. The SFC is an excellent indicator of the optimal cycle and can be used to compare SGT, GT-ABC, and POGT. As a result, the cycle with the lowest SFC is more valuable than the others. Plotting the TIT against the SFC (Figure 6) at the same operational data revealed that the SFC of each cycle decreases with increased TIT reach about stable conditions at certain TIT., which may be attributed to the significant gain in thermal efficiency with TIT. According to the variation of TIT, The SFC of GT-ABC is higher than that for SGT and POGT. There is a significant difference, specifically in the low range of TIT. There is a minor difference between The SFC of SGT and GT-ABC.

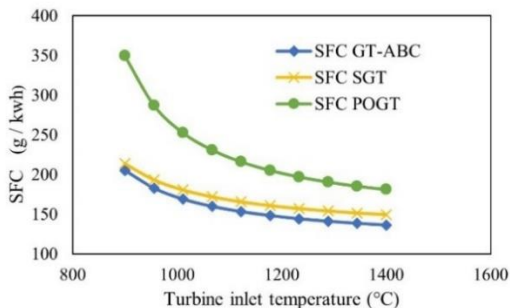


Figure 6. Specific fuel consumption (SFC) variation against turbine inlet temperature ($R_c = 20$, $T_o = 25^\circ\text{C}$, $x = 0.2$ and $r_c = 2$).

4.1.3 Effect of Compression Ratio on Energy and Exergy Efficiencies

The pressure ratio was changed between 2 and 35; increasing the compression ratio in gas turbine cycles increases the energy and exergy efficiencies. Similar trends were observed for SGT, GT-ABC, and POGT, as seen from the presented data in Figure 7. The findings show that the energy and exergy efficiencies will decrease for each cycle at low and high-pressure ratios (below or above the design condition). The optimum pressure ratio for SGT is 24, corresponding to 42.2%, 39.8% energy, and exergy efficiencies, respectively. In contrast, the optimum pressure ratio for GT-ABC is 30, corresponding to 39.7% and 36.8% energy and exergy efficiency, respectively. In addition, the optimum pressure ratio for POGT is 13, corresponding to energy and exergy efficiencies of 42.5% and 40.7 %,

respectively. The energy and exergy efficiencies of SGT increase between 20% and 40% sharply in the low compression ratio range between 2 and 13. Then, the efficiencies grow gradually in the higher range of compression ratio between 13 and 30. While in the low compression ratio range of 2 to 10, the energy and exergy efficiencies of GT-ABC improved sharply between 15% and 30%. The efficiencies gradually rise in the higher compression ratio range of 10 to 30. In contrast, the energy and exergy efficiencies of POGT increase significantly between 30% and 42% in the low compression ratio range of 2 to 13. The efficiencies gradually decrease in the higher compression ratio range of 13 to 30.

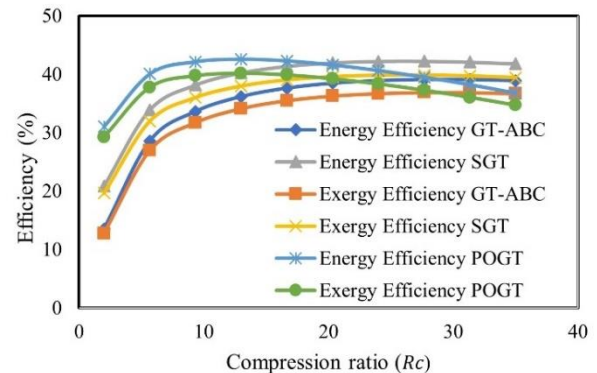


Figure 7. Energy and exergy efficiencies variation with compression ratio ($TIT = 1400^\circ\text{C}$, $T_o = 25^\circ\text{C}$, $x = 0.2$ and $r_c = 2$).

4.1.4 Effect of Compression Ratio on Specific Fuel Consumption

Figure 8 illustrates the effect of compression ratio on SFC for SGT, GT-ABC, and POGT cycles. The general trend is similar for each cycle. The SFC reduces significantly in the compression ratio range between 2 and 6, then stabilizes in the compression ratio range between 6 and 35. For the low range of compression ratio, the SFC for POGT is lower than other cycles, while at the high range of compression ratio, the SFC for SGT is lower than different cycles, reaching around 130 g/kwh.

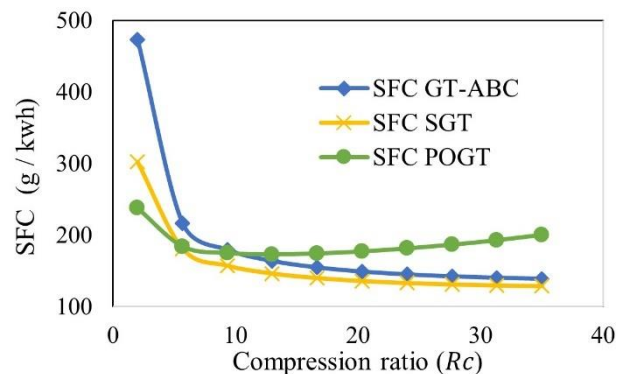


Figure 8. Specific fuel consumption (SFC) variation against compression ratio ($TIT = 1400^\circ\text{C}$, $T_o = 25^\circ\text{C}$, $x = 0.2$ and $r_c = 2$).

4.1.5 Effect of Ambient Air Temperature on Energy and Exergy Efficiencies

To investigate the impact of environmental conditions on the operation of each cycle., the ambient temperature varied from 5 °C to 35 °C. Figure 9 illustrates how the energy and exergy efficiencies change as a function of ambient

temperature for the SGT, GT-ABC, and POGT. Increased ambient temperature decreases energy and exergy efficiencies for all cycles. It is revealed that the POGT has higher energy and exergy efficiencies than the other cycle. Moreover, it declines because of a rise in ambient temperature. For example, at $T_o = 5\text{ }^\circ\text{C}$, the energy efficiency of SGT, GT-ABC, and POGT was 39.6%, 41.4, and 41.3 %, respectively, while the exergy efficiency was 37.3%, 39.1%, and 40.9%. In contrast, at $T_o = 35\text{ }^\circ\text{C}$, the energy efficiency of SGT, GT-ABC, and POGT were 37.7%, 39.2%, and 40.7%, respectively, while the exergy efficiencies were 35.5%, 37 %, and 38.4%. As shown in Figure 9 even while the POGT has higher overall efficiency than the SGT, GT-ABC, the rate at which efficiency decreases with ambient temperature in the basic cycle is lower.

4.1.6 Effect of Ambient Air Temperature on Specific Fuel Consumption

The specific fuel consumption SFC shows the quantity of fuel required to produce a certain level of power. The work that the gas turbine reduces as the ambient temperature increases. As a result, the SFC of the gas turbine increases. For all cycles, the SFC of the gas turbine cycle increases with the ambient air temperature. Significant variation was revealed for the POGT, as shown in Figure 10. It proves that at a fixed compression ratio, a rise in intake air temperature leads to a rise in fuel consumption. This can be interpreted as follows; as the ambient temperature declines, the air mass flow rate at the compressor input rises, resulting in a reduction in SFC.

A comprehensive quantitative comparison of the SGT, GT-ABC, and POGT is given in Table 5. The values of overall energy and exergy efficiencies and SFC according to an extensive range of operating conditions are shown. The

table shows that under all low-pressure ratio values (8 to 20), the POGT cycle has higher energy and exergy performance than the SGT, GT-ABC, and GT-ABC cycles.

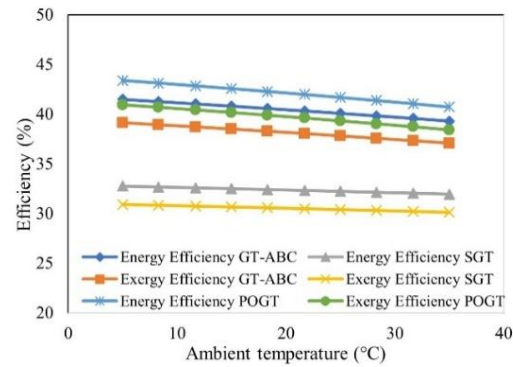


Figure 9. Variation of energy and exergy efficiency with the ambient condition ($TIT = 1400\text{ }^\circ\text{C}$, $R_c = 20$, $x = 0.2$ and $rc = 2$).

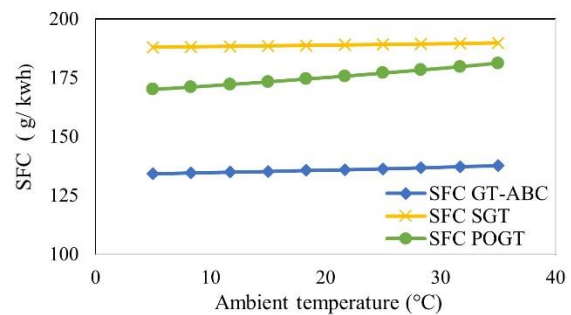


Figure 10. Specific fuel consumption (SFC) variation against ambient temperature ($TIT = 1400\text{ }^\circ\text{C}$, $R_c = 20$, $x = 0.2$ and $rc = 2$).

Table 5. Overall efficiency and Specific fuel consumption (SFC) for different values of TIT , T_o , and R_c associated with the SGT, GT-ABC, and POGT cycles. (The pressure ratio of the bottoming cycle for GT-ABC is $rc = 2$, and the mass fraction for POGT is $x = 0.2$).

$TIT\text{ (}^\circ\text{C)}$	$T_o\text{ (}^\circ\text{C)}$	R_c	Simple-GT			GT-ABC			POGT		
			Energy efficiency (%)	Exergy efficiency (%)	SFC (g/kwh)	Energy efficiency (%)	Exergy efficiency (%)	SFC (g/kwh)	Energy efficiency (%)	Exergy efficiency (%)	SFC (g/kwh)
900	5	8	27.77	26.2	215.5	30.12	28.41	191.9	40.54	38.24	182
		20	27.71	26.14	190.7	28.12	26.53	179.5	30.35	28.63	243.1
		30	21.82	20.58	215.6	21.25	20.05	207.9	15.8	14.91	215.6
	25	8	26.44	24.94	221.7	28.35	26.75	199.3	39.81	37.56	185.3
		20	23.38	22.06	213.8	23.08	21.77	205.2	24.65	23.25	299.3
		30	13.18	12.44	324.7	11.54	10.88	333.7	2.115	1.995	324.7
	35	8	25.69	24.24	225.6	27.37	25.82	203.8	39.38	37.15	187.3
		20	20.75	19.57	233.2	20.01	18.88	227.4	21.1	19.9	349.6
		30	7.426	7.006	570.3	5.066	4.779	686.6	7.366	6.949	570.3
1200	5	8	31.47	29.69	194.4	34.71	32.74	169.3	41.7	39.34	176.9
		20	36.83	34.74	155.3	38.43	36.25	142.4	40.37	38.09	182.7
		30	36.82	34.74	148	37.8	35.66	137.4	36.22	34.17	203.7
	25	8	30.75	29.01	196.4	33.77	31.85	171.7	41.25	38.91	178.8
		20	35.04	33.06	159.2	36.35	34.3	146.5	37.95	35.8	194.4
		30	34	32.08	154.5	34.63	32.67	144	31.82	30.02	231.8
	35	8	30.37	28.65	197.6	33.26	31.37	173.1	40.98	38.66	180
		20	34.04	32.11	161.7	35.19	33.2	149.1	36.56	34.49	201.8
		30	32.36	30.52	159	32.79	30.93	148.5	29.2	27.55	252.6
1400	5	8	32.75	30.9	187.9	36.25	34.2	162.3	42.04	39.66	175.5
		20	39.62	37.38	147.4	41.48	39.13	134.2	43.37	40.92	170.1
		30	40.9	38.59	138	42.17	39.78	127.3	41.55	39.19	177.5
	25	8	32.22	30.39	189.1	35.55	33.54	163.7	41.66	39.3	177
		20	38.4	36.23	149.5	40.07	37.8	136.3	41.67	39.31	177
		30	39.1	36.88	141	40.15	37.88	130.2	38.7	36.51	190.6
	35	8	31.93	30.12	189.8	35.17	33.18	164.5	41.45	39.1	178
		20	37.73	35.59	150.7	39.29	37.07	137.6	40.71	38.41	181.2
		30	38.08	35.92	142.8	39.01	36.8	132.1	37.06	34.96	199

5. Conclusion:

In this article, a comparative study was conducted based on energy and exergy analysis for SGT, GT-ABC, and POGT cycles to determine the most effective system, along with the developed model and EES software that has been used to evaluate the effect of critical operational parameters. The main results observed from the study are summarized below:

- The parametric analysis showed that the ambient temperature, turbine inlet temperature, and compression ratio significantly affected the energy and exergy efficiencies of SGT, GT-ABC, and POGT cycles.
- As the compression ratio grows, the energy and exergy efficiencies of the SGT, GT-ABC, and POGT cycles also increase.
- The energy and exergy efficiencies of each cycle will degrade at low- and high-pressure ratios (below or above the design condition). The optimum pressure ratio for SGT is 24, corresponding to 42.2%, 39.8% energy, and exergy efficiencies, respectively. In contrast, the optimum pressure ratio for GT-ABC is 30, related to 39.7% and 36.8% energy and exergy efficiency, respectively. In addition, the optimum pressure ratio for POGT is 13, corresponding to 42.5% and 40.7 % energy and exergy efficiencies, respectively.
- There is an optimum TIT at which each cycle's energy and exergy efficiencies are at their highest values for all pressure ratios.
- Comprehensive modelling shows that the POGT cycle can achieve higher efficiency at the same turbine inlet temperature and pressure ratio. The model findings indicate that when the ambient temperature rises, the total efficiency of all cycles decreases.
- For all cycles, at (TIT = 1400 °C, T_o = 25 °C, R_c = 20, x=0.2 and r_c = 2), the GT-ABC and POGT cycles are more efficient than that SGT. Under these conditions, the energy and exergy efficiency are 38.4%, 36.2% for SGT, 40%, 37.8 % for GT-ABC, and 41.6%, 39.3% for POGT. In addition, the SFC for SGT, GT-ABC, and POGT cycles is 149.5, 136.3, and 177 (g/kwh), respectively.
- Finally, in all low-pressure ratio conditions (8 to 20), the POGT cycle has a higher energy and exergy performance than the SGT, GT-ABC.

Nomenclature

Symbols

C_p	Specific heat (kJ/kg.)
h	Specific enthalpy (J/kg)
\dot{m}	Mass flow rate (kg/s)
P	Pressure (kPa)
q	Heat supplied (W)
R_c	Pressure ratio in topping cycle
r_c	Pressure ratio in bottoming cycle
s	Specific entropy (J/kg. K)
T	Temperature (K)
W	Work (W)

Abbreviation

AF	Air-to-fuel ratio
CIT	Compressor inlet temperature
GT-ABC	Gas turbine with air bottoming cycle
LHV	Fuel lower heating value (kJ/kg)
NG	Natural gas
SGT	Simple gas turbine
SFC	Specific fuel consumption (g/wh)
TIT	Turbine inlet temperature (k)
POGT	Partial oxidation gas turbine

Subscripts

a	Air
B	Bottoming cycle
c	Compressor
cc	Combustion chamber
GT	Gas turbine
net	Net
o	Outlet
p	Pump
T	Topping cycle

Greek Symbols

η	Thermal efficiency
ϵ	Effectiveness of HE
γ	Ratio of specific heat

References:

- [1] J. A. M. da Silva, S. Ávila Filho, and M. Carvalho, "Assessment of energy and exergy efficiencies in steam generators," *Journal of the Brazilian Society of Mechanical Sciences and Engineering*, vol. 39, no. 8, pp. 3217–3226, 2017, doi: 10.1007/s40430-016-0704-6.
- [2] M. N. Ibrahim, T. K., Mohammed, M. K., Awad, O. I., Abdalla, A. N., Basrawi, F., Mohammed, "A comprehensive review on the exergy analysis of combined cycle power plants," *Renewable and Sustainable Energy Reviews*, vol. 90, no. April, pp. 835–850, Jul. 2018, doi: 10.1016/j.rser.2018.03.072.
- [3] A. G. Memon, R. A. Memon, K. Harijan, and M. A. Uqaili, "Thermo-environmental analysis of an open cycle gas turbine power plant with regression modeling and optimization," *Journal of the Energy Institute*, vol. 87, no. 2, pp. 81–88, 2014, doi: 10.1016/j.joei.2014.03.023.
- [4] Ş. Balku, "Analysis of combined cycle efficiency by simulation and optimization," *Energy Conversion and Management*, vol. 148, pp. 174–183, Sep. 2017, doi: 10.1016/j.enconman.2017.05.032.
- [5] O. J. Khaleel, F. Basim Ismail, T. Khalil Ibrahim, and S. H. bin Abu Hassan, "Energy and exergy analysis of the steam power plants: A comprehensive review on the Classification, Development, Improvements, and configurations," *Ain Shams Engineering Journal*, vol. 13, no. 3, p. 101640, 2022, doi: 10.1016/j.asej.2021.11.009.
- [6] D. M. Mitrović, B. V. Stojanović, J. N. Janevski, M. G. Ignjatović, and G. D. Vučković, "Exergy and exergoeconomic analysis of a steam boiler," *Thermal Science*, vol. 22, pp. S1601–S1612, 2018, doi: 10.2298/TSCI18S5601M.
- [7] G. R. Ahmadi and D. Toghraie, "Energy and exergy analysis of Montazeri Steam Power Plant in Iran," *Renewable and Sustainable Energy Reviews*, vol. 56, pp. 454–463, 2016, doi: 10.1016/j.rser.2015.11.074.
- [8] O. K. Singh, "Assessment of thermodynamic irreversibility in different zones of a heavy fuel oil fired high pressure boiler," *Journal of Thermal Analysis and Calorimetry*, vol. 123, no. 1, pp. 829–840, 2016, doi: 10.1007/s10973-015-4959-4.
- [9] M. Hajzadeh aghdam, M. H. Khoshgoftar manesh, N. Khani, and M. Yazdi, "Energy, Exergy-Based and Emergy-Based Analysis of Integrated Solar PTC with a Combined Cycle Power Plant," *International Journal of Thermodynamics*, vol. 24, no. 4, pp. 17–30, Dec. 2021, doi: 10.5541/ijot.902374.

- [10] S. Zandi, K. G. Mofrad, A. Moradifaraj, and G. R. Salehi, "Energy, exergy, exergoeconomic, and exergoenvironmental analyses and multi-objective optimization of a CPC driven solar combined cooling and power cycle with different working fluids," *International Journal of Thermodynamics*, vol. 24, no. 2, pp. 151–170, May 2021, doi: 10.5541/ijot.873456.
- [11] M. R. Abedi, G. Salehi, M. T. Azad, M. H. K. Manesh, and H. Fallahsohi, "Exergetic and exergoeconomic analysis and optimization of gas turbine inlet air cooling systems with absorption or compression chilling," *International Journal of Thermodynamics*, vol. 24, no. 2, pp. 93–107, 2021, doi: 10.5541/ijot.785357.
- [12] R. Yildirim, A. Şencanşahin, and E. Dikmen, "Comparative Energetic, Exergetic, Environmental and Enviroeconomic Analysis of Vapour Compression Refrigeration Systems Using R515B as Substitute for R134a," *International Journal of Thermodynamics*, vol. 25, no. 1, pp. 125–133, Mar. 2022, doi: 10.5541/ijot.1011622.
- [13] A. K. Mahapatra and Sanjay, "Performance analysis of an air humidifier integrated gas turbine with film air cooling of turbine blade," *Journal of Energy in Southern Africa*, vol. 24, no. 4, pp. 71–81, 2013, doi: 10.17159/2413-3051/2013/v24i4a3148.
- [14] A. M. Alklaibi, M. N. Khan, and W. A. Khan, "Thermodynamic analysis of gas turbine with air bottoming cycle," *Energy*, vol. 107, no. x, pp. 603–611, 2016, doi: 10.1016/j.energy.2016.04.055.
- [15] F. Y. Ibrahim, T. K., Basrawi, F., Awad, O. I., Abdullah, A. N., Najafi, G., Mamat, R., & Hagos, "Thermal performance of a gas turbine based on an exergy analysis," *Applied Thermal Engineering journal*, vol. 128, p. 01027, Nov. 2019, doi: 10.1051/e3sconf/201912801027.
- [16] H. Kurt, Z. Recebli, and E. Gedik, "Performance analysis of open cycle gas turbines," *International Journal of Energy Research*, vol. 33, no. 3, pp. 285–294, Mar. 2009, doi: 10.1002/er.1472.
- [17] A. De Sa and S. Al Zubaidy, "Gas turbine performance at varying ambient temperature," *Applied Thermal Engineering*, vol. 31, no. 14–15, pp. 2735–2739, 2011, doi: 10.1016/j.applthermaleng.2011.04.045.
- [18] M. M. Abou Al-Sood, K. K. Matrawy, and Y. M. Abdel-Rahim, "Optimum Operating Parameters of an Irreversible Gas Turbine Cycle," *JES. Journal of Engineering Sciences*, vol. 40, no. 6, pp. 1695–1714, 2012, doi: 10.21608/jesaun.2012.114611.
- [19] H. Aydin, "Exergetic sustainability analysis of LM6000 gas turbine power plant with steam cycle," *Energy*, vol. 57, pp. 766–774, 2013, doi: 10.1016/j.energy.2013.05.018.
- [20] C. Carcasci, F. Costanzi, and B. Pacifici, "Performance Analysis in Off-Design Condition of Gas Turbine Air-Bottoming Combined System," *Energy Procedia*, vol. 45, pp. 1037–1046, 2014, doi: 10.1016/j.egypro.2014.01.109.
- [21] M. Ghazikhani, I. Khazaei, and E. Abdekhodaie, "Exergy analysis of gas turbine with air bottoming cycle," *Energy*, vol. 72, pp. 599–607, 2014, doi: 10.1016/j.energy.2014.05.085.
- [22] M. Ghazikhani, H. Takdehghan, and A. M. Shayegh, "Exergy Analysis of Gas Turbine Air- Bottoming Combined Cycle for Different Environment Air Temperature," *Proceedings of 3rd International Energy, Exergy and Environment Symposium*, no. November, pp. 1–8, 2007.
- [23] J. Rabovitser, S. Nester, S. Wohadlo, K. Smith, W. Nazeer, and D. White, "Development of a partial oxidation gas turbine (POGT) for innovative gas turbine systems," *Proceedings of the ASME Turbo Expo*, vol. 3, pp. 261–269, 2007, doi: 10.1115/GT2007-27539.
- [24] S. J. Zhang, J. L. Chi, and Y. H. Xiao, "Performance analysis of a partial oxidation steam injected gas turbine cycle," *Applied Thermal Engineering*, vol. 91, no. x, pp. 622–629, 2015, doi: 10.1016/j.applthermaleng.2015.08.062.
- [25] C. Diyoke, U. Ngwaka, and T. O. Onah, "Comparative assessment of a hybrid of gas turbine and biomass power system for sustainable multi-generation in Nigeria," *Scientific African*, vol. 13, 2021, doi: 10.1016/j.sciaf.2021.e00899.
- [26] Y. Fan, G., Lu, X., Chen, K., Zhang, Y., Han, Z., Yu, H., & Dai, "Comparative analysis on design and off-design performance of novel cascade CO₂ combined cycles for gas turbine waste heat utilization," *Energy*, vol. 254, 2022, doi: 10.1016/j.energy.2022.124222.
- [27] B. R. Ryu, P. A. Duong, and H. Kang, "Comparative analysis of the thermodynamic performances of solid oxide fuel cell–gas turbine integrated systems for marine vessels using ammonia and hydrogen as fuels," *International Journal of Naval Architecture and Ocean Engineering*, vol. 15, 2023, doi: 10.1016/j.ijnaoe.2023.100524.
- [28] J. Yi, "Design and optimization of gasoline direct injection engines using computational fluid dynamics," *Advanced Direct Injection Combustion Engine Technologies and Development: Gasoline and Gas Engines*, pp. 166–198, Oct. 2009, doi: 10.1533/9781845697327.166.
- [29] R. Kumar, "A critical review on energy, exergy, exergoeconomic and economic (4-E) analysis of thermal power plants," *Engineering Science and Technology, an International Journal*, vol. 20, no. 1, pp. 283–292, Feb. 2017, doi: 10.1016/j.jestch.2016.08.018.
- [30] E. Ersayin and L. Ozgener, "Performance analysis of combined cycle power plants: A case study," *Renewable and Sustainable Energy Reviews*, vol. 43, pp. 832–842, 2015, doi: 10.1016/j.rser.2014.11.082.
- [31] C. Michalakakis, J. Fouillou, R. C. Lupton, A. Gonzalez Hernandez, and J. M. Cullen, "Calculating the chemical exergy of materials," *Journal of Industrial Ecology*, vol. 25, no. 2, pp. 274–287, Apr. 2021, doi: 10.1111/jiec.13120.
- [32] M. Maheshwari and O. Singh, "Comparative evaluation of different combined cycle configurations having simple gas turbine, steam turbine and ammonia water turbine," *Energy*, vol. 168, pp. 1217–1236, Feb. 2019, doi:

10.1016/j.energy.2018.12.008.

- [33] M. Ghazikhani, I. Khazaei, and E. Abdekhodaie, "Exergy analysis of gas turbine with air bottoming cycle," *Energy*, vol. 72, pp. 599–607, 2014, doi: 10.1016/j.energy.2014.05.085.
- [34] D. Rabovitser, J., Wohadlo, S., Pratapas, J. M., Nester, S., Tartan, M., Palm, S., ... & White, "Experimental Study of a 200 kW Partial Oxidation Gas Turbine (POGT) for Co-Production of Power and Hydrogen-Enriched Fuel Gas," in *Volume 4: Cycle Innovations; Industrial and Cogeneration; Manufacturing Materials and Metallurgy; Marine*, Jan. 2009, vol. 4, pp. 133–145, doi: 10.1115/GT2009-59272.
- [35] M. A. Korobitsyn, P. W. Kers, and G. G. Hirs, "Analysis of a gas turbine cycle with partial oxidation," *Proceedings of the ASME Turbo Expo*, vol. 3, 1998, doi: 10.1115/98-GT-033.
- [36] Y. S. H. Najjar and M. S. Zaamout, "Performance analysis of gas turbine air-bottoming combined system," *Energy Conversion and Management*, vol. 37, no. 4, pp. 399–403, 1996, doi: 10.1016/0196-8904(95)00197-2.
- [37] M. N. Khan and I. Tlili, "New approach for enhancing the performance of gas turbine cycle: A comparative study," *Results in Engineering*, vol. 2, no. February, p. 100008, 2019, doi: 10.1016/j.rineng.2019.100008.
- [38] M. N. Khan, I. M. Alarifi, and I. Tlili, "Comparative energy and exergy analysis of proposed gas turbine cycle with simple gas turbine cycle at same operational cost," *ASME International Mechanical Engineering Congress and Exposition, Proceedings (IMECE)*, vol. 6, no. February 2022, 2019, doi: 10.1115/IMECE2019-10949.